Optik 125 (2014) 3217–3220

Contents lists available at ScienceDirect

Optik

journal homepage: www.elsevier.de/ijleo

Study on the photovoltaic property of Cu_4SnS_4 synthesized by mechanochemical process

Qinmiao Chen [a], Xiaoming Dou [a,b,d,*], Zhenqing Li [a], Yi Ni [a], Jin Chen [a], Fangfang Zhou [a], Yoshinori Yamaguchi [a,c], Songlin Zhuang [a]

[a] Engineering Research Center of Optical Instrument and System (Ministry of Education), Shanghai Key Laboratory of Modern Optics System, School of Optical-Electrical and Computer Engineering, University of Shanghai for Science and Technology, 516 Jungong Road, Shanghai 200093, People's Republic of China
[b] Department of Physics, Shanghai Jiao Tong University, 800 Dongchuan Road, Minhang District, Shanghai 200240, People's Republic of China
[c] Photonics Advanced Research Center, Graduate School of Engineering, Osaka University, 2-1, Yamadaoka, Suita-city, Osaka 565-0871, Japan
[d] Consolidated Research Institute for Advanced Science and Medical Care, Waseda University, 513 Wasedatsurumaki-cho, Shinjuku-ku, Tokyo 162-0041, Japan

ARTICLE INFO

Article history:
Received 25 June 2013
Accepted 16 December 2013

Keywords:
Inorganic compounds
Cu_4SnS_4
Photovoltaic property

ABSTRACT

Photovoltaic property of Cu_4SnS_4 (CTS) is studied by employing a superstrate solar cell structure of Mo/CTS/In_2S_3/TiO_2/fluorine-doped tin oxide (FTO) glass for the first time. The CTS absorber layer was prepared by a combination of mechanochemical and doctor blade processes. The annealing effects on the structural, optical and electronic properties of the CTS absorber layer were investigated. The novel CTS absorber layer shows conversion efficiency as high as 2.34% under the standard AM 1.5 condition.

1. Introduction

Thin film of chalcopyrite $CuIn_xGa_{1-x}(S,Se)_2$ (CIGS) has attracted a lot of attention as solar cell absorber layer because of its large absorption coefficient (10^5 cm^{-1}), tunable bandgap (1.04–1.7 eV), high stability and demonstrated high solar cell conversion efficiency (>20%) [1–3]. However, the constituent element In of the CIGS is abundantly low in the crust of the earth (0.049 ppm) [4], together with the competition for it from the flat panel display industry, making the cost of the CIGS very high. In addition, the constituent element Se is also toxic. Therefore, developing new photovoltaic absorber layer materials free of scarce and toxic elements is extremely important for large-scale solar cell production in the near future.

Tin (Sn) is nontoxic and its content is abundant in the crust of the earth (Sn: 2.2 ppm [4]), which makes Sn-based compounds Cu_2ZnSnS_4 (CZTS) and those in the Cu–Sn–S system promising photovoltaic absorber layer materials for the production of cheaper large-area thin film solar cell modules for the terawatt-year level production of electric energy. Solar cell employing CZTS as absorber layer has reached 6.7% conversion efficiency from the conventional substrate structure of Al/ZnO:Al/ZnO/CdS/CZTS/Mo/glass [5]. Cu–Sn–S system compounds [6,7], such as Cu_4SnS_4 (CTS) or Cu_2SnS_3 [8–12], were also reported as promising candidates for photovoltaic application because of their excellent optical and electronic properties. However, the photovoltaic properties of these ternary compounds are studied rarely.

In the present study, the photovoltaic property of CTS is reported for the first time. In order to study the photovoltaic property of the CTS, a superstrate solar cell structure of Mo/CTS/In_2S_3/TiO_2/fluorine-doped tin oxide (FTO) glass, developed previously by our Lab with simple and low-cost non-vacuum technologies, was employed [13]. The CTS absorber layer was prepared by a combination of mechanochemical and doctor blade processes. The annealing effects on the structural, optical and electrical properties of the CTS absorber layer were investigated.

2. Experimental method

CTS powder was synthesized by simple mechanochemical ball milling process [14]. In order to investigate the photovoltaic properties of the CTS, a simple superstrate solar cell structure of Mo/CTS/In_2S_3/TiO_2/FTO glass previously developed by our Lab was

* Corresponding author at: Room 206, Department of Physics, Shanghai Jiao Tong University, 800 Dongchuan Road, Minhang District, Shanghai 200240, People's Republic of China. Tel.: +86 21 55276023; fax: +86 21 54745803.
E-mail address: xiaomingdou@yeah.net (X. Dou).

0030-4026/$ – see front matter © 2014 Elsevier GmbH. All rights reserved.
http://dx.doi.org/10.1016/j.ijleo.2013.12.023

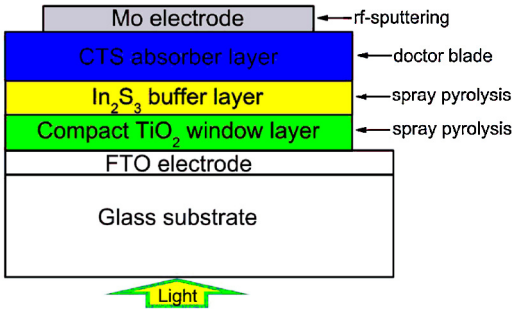

Fig. 1. Structure of the solar cell.

employed. The fabrication process of the solar cell was presented in the following.

2.1. Synthesis of CTS material

Simple ball milling process was applied for the synthesis of CTS material. Element powders copper (Cu; 99.9%, Wako Chemicals), tin (Sn; 99.5%, Aldrich) and sulfur (S; 99.9%, Kishida Chemicals) were mixed in molar ratio of 4:1:4. The mixture was then milled by the planetary ball miller at various rotation speeds for 1 h to obtain completely reacted production. A rotation speed of 800 rpm was realized as suitable condition for this purpose (detailed data not shown here).

2.2. Fabrication of the solar cell

The structure of the solar cell is depicted in Fig. 1. The corresponding thin film layers of the solar cell were prepared as follows.

2.2.1. Deposition of compact TiO_2 window layer and In_2S_3 buffer layer

Both of compact TiO_2 window layer and In_2S_3 buffer layer were prepared by spray pyrolysis method [15,16]. Briefly, for compact TiO_2 window layer, titanium isopropoxide and acetylacetone were mixed with a molar ration of 0.5 (named TAA). The mixture solution was further diluted by ethanol (TAA:ethanol = 1:9 (v/v)) to make spray solution. Prior to spray, the FTO glass substrate (10 cm × 10 cm) was ultrasonically cleaned, sequentially in acetone, distilled water and ethanol for 15 min. The FTO glass was then treated by UV/O_3 cleaner (PL16-110, Sen Lights Corporation) for 20 min to remove some organic dust on the FTO surface. The substrate temperature was kept at 450 °C during spraying, and 50 ml spray solution was employed for compact TiO_2 window layer deposition. For In_2S_3 buffer layer, 50 ml aqueous solution with 0.01 M $InCl_3$ (98%, Tokyo Chemicals, anhydrous) and 0.06 M thiourea was employed, where additional thiourea was intentionally used for getting sulfur rich buffer layer. The CTS absorber layer was grown on the buffer layer, thus the sulfur rich buffer layer could benefit to the quality improvement of the CTS absorber layer during annealing process. Before In_2S_3 buffer layer spray, the compact TiO_2 window layer was treated with 40 mM $TiCl_4$ aqueous solution (1.50–1.69 mg/ml, Wako Chemicals Inc.) at 70 °C for 30 min to smoothen the film. The substrate temperature for the buffer layer spray was 200 °C. The thicknesses of the deposited compact TiO_2 window layer and In_2S_3 buffer layer were about 100 and 300 nm, respectively.

2.2.2. Preparation of CTS paste

CTS paste was prepared in a milling motor: (1) 0.2 g CTS powder was first grinded alone for 5 min; (2) 1 ml 10 wt% thiourea aqueous solution was then slowly added while keeping grinding for another 10 min; (3) finally, 2 ml propylene glycol (Kando Chemicals) was slowly added while keeping grinding for 10 min. The milling time for each step may be slightly changed for getting doctor blade paste with desirable viscosity.

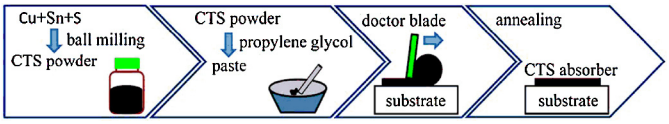

Fig. 2. Preparation scheme of CTS absorber layer.

2.2.3. Deposition of CTS absorber layer

CTS paste was deposited on pre-prepared In_2S_3/TiO_2/FTO glass substrates by doctor blade method [17]. After being dried in air at 125 °C for 5 min, the samples (CTS/In_2S_3/TiO_2/FTO glass) were annealed in N_2 ambience to improve the crystallinity of the CTS. A preparation scheme of the CTS absorber layer is shown in Fig. 2.

2.2.4. Deposition of Mo electrode

Finally, Mo electrodes were sputtered on the annealed samples (CTS/In_2S_3/TiO_2/FTO glass) to complete the CTS solar cell fabrication (Mo/CTS/In_2S_3/TiO_2/FTO glass). The active area of the solar cell is 0.5 cm × 0.5 cm.

2.3. Characterization methods

Crystallinity and phase composition of the CTS absorber layers (CTS/In_2S_3/TiO_2/FTO glass) were confirmed by X-ray diffraction spectrometer (XRD; MiniFlex 600 Rigaku). Sample morphology was observed by scanning electron microscope (SEM; JSM-6510, JEOL). UV–vis-IR absorption spectra were measured in absorbance spectroscopy by spectrophotometer (Lambda 750, PerkinElmer). Photovoltaic measurement of the completed solar cell was performed under an AM 1.5 solar simulator equipped with a xenon lamp (YSS-100A, Yamashita Denso). The power of the simulated light was calibrated to 100 mW/cm^2 by using a reference Si photodiode (Bunkou Keiki). *J–V* (short-circuit current density J_{sc} and open-circuit voltage V_{oc}) curves were obtained by applying an external bias to the cell and measuring the generated photocurrent with an APCMT 6240 DC voltage current source.

3. Results and discussion

3.1. XRD analysis

To confirm the crystallinity and phase composition of the CTS absorber layer, XRD measurements were performed. Fig. 3 depicts the XRD patterns of the CTS absorber layers prepared at various

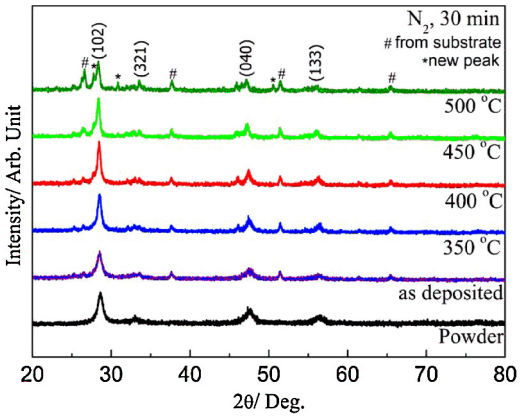

Fig. 3. XRD patterns of CTS absorber layers prepared at various temperatures.

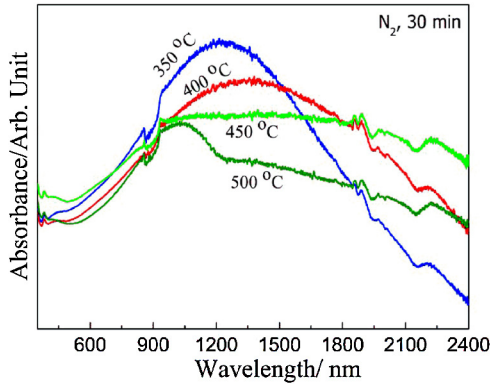

Fig. 4. UV–vis-IR absorption spectra of CTS absorber layers prepared at various temperatures.

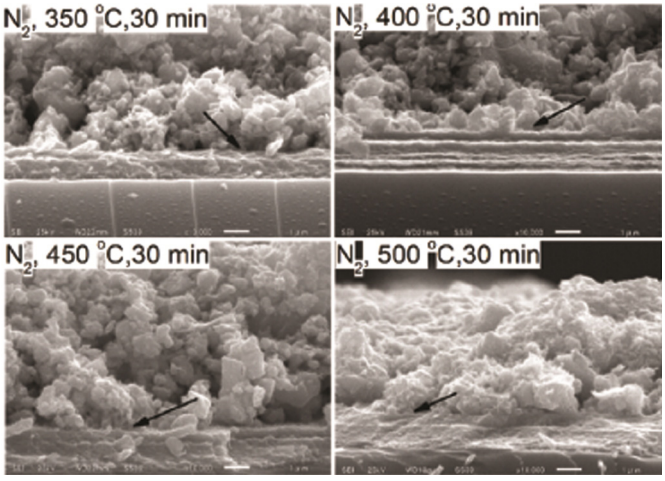

Fig. 5. SEM cross-section images of CTS absorber layers and p–n junction interfaces prepared at various temperatures.

annealing temperatures. The XRD pattern of the as deposited CTS absorber layer at the positions of 28.6, 33.1, 47.7 and 56.5° are assigned to CTS (1 0 2), (3 2 1), (0 4 0) and (1 3 3) (PDF #290584), respectively. The diffraction peaks of the as deposited sample are weak and broad. However, after annealing, the XRD peaks become sharp and strong compared with those of the as deposited sample. The sharp and strong peaks can be attributed to the improved crystallinity of the CTS by the annealing process.

However, when annealing, the temperature reached 500 °C; the XRD peak intensity (specially the (1 0 2)) is distinctly decreased and many new peaks that do not belong to the CTS appear. The new peaks at 27.7, 30.8 and 50.6° could be assigned to Cu_2S (2 6 2), (0 9 1) and (5 9 3) (PDF #230961), respectively. This deterioration may be due to the evaporation of Sn and S atoms or decomposition of the CTS by the high temperature annealing [18–20]. As a result, for the CTS absorber layer, the annealing temperature should be below 500 °C.

3.2. UV–vis-IR analysis

In order to investigate the annealing effects on the optical properties of the CTS absorber layer, we measured the UV–vis-IR absorption spectra (Fig. 4) of the annealed samples. As shown in Fig. 4, the absorption characteristics of the annealed samples at long wavelength (>935 nm) strongly depend on the annealing temperatures. The absorption intensity decreases as the annealing temperature increases at wavelength range between 935 and 1500 nm, whereas, the absorption intensity generally increases with the increased annealing temperature at wavelength longer than 1500 nm. Therefore, the CTS could be sensitive to the annealing temperature.

In addition, by using a simple bandgap value (E_g) measurement method of $E_g = h \times C/\lambda$ (h is the Planck's constant, C is the speed of light, and λ is the absorption cutoff wavelength that can be obtained from the absorption spectra), the calculated bandgap value of the sample annealed at 350 °C is about 0.55 eV. The compound material with bandgap value of 0.55 eV has potential application in high-efficiency 3- and 4-junction thin-film solar cell [21]. The bandgap of the annealed sample becomes smaller as the annealing temperature is further increased. In addition, the absorption curve, the sample annealed at 500 °C, turns out very different (at wavelength range between 935 and 1500 nm) compared to that of the other samples. In the sample annealed at 500 °C, there appears an additional absorption shoulder at 1214.3 nm, which indicates that material with bandgap value of 1.02 eV springs out after the high temperature annealing. The CTS is reported as a compound of joint Cu_2S–SnS_2 [22]; thus, the compound annealed in N_2 ambience at 500 °C may partly decompose into SnS_2 and Cu_2S. The SnS_2 may evaporate away, and the Cu_2S may remain with an element deviated formation since its bandgap is just 1.02 eV (reported bandgap value for Cu_2S is about 1.2 eV [23]). These discussions are consistent with the XRD result.

3.3. SEM morphology observation

Fig. 5 shows the SEM cross-section images of CTS absorber layers and p–n junction interfaces prepared at various temperatures. As can be seen in the images, the density of the annealed CTS absorber layer is rather good, while, the film is still powder-like. Among the prepared samples, the morphology of the sample annealed at 500 °C turns out significant difference compared with that of the other samples, which may be due to the decomposition of the CTS as discussed in the XRD and UV–vis-IR data. In addition, the p–n junction interface between the CTS absorber layer and the In_2S_3 buffer layer might be rough since the CTS absorber layer is powder-like. However, there are few gaps in the p–n junction interface, which may be due to the reaction at the interface between the wide-bandgap In_2S_3 buffer layer (above 2.0 eV) and the CTS absorber layer during the annealing process [24]. The good p–n junction interface would benefit to the photovoltaic characteristics of the solar cell.

3.4. J–V photoelectric characteristics analysis

For analyzing the photoelectric conversion properties of the CTS absorber layer, completed solar cells with superstrate structure of Mo/CTS/In_2S_3/TiO_2/FTO glass were fabricated. J–V characteristics of the samples annealed at various temperatures (350, 400, 450 and 500 °C) are shown in Fig. 6 (solar cell parameters are summarized in Table 1). As shown in Fig. 6, the J_{sc} of the solar cell increases as the annealing temperature increases from 350 to 400 °C. However, it significantly decreases when the temperature is further increased to 450 or 500 °C, which may be due to the deterioration

Table 1
Solar cell parameters summarized from Fig.6.

Annealing temperature (°C)	J_{sc} (mA/cm^2)	V_{oc} (V)	FF	Efficiency (%)
350	17.44	0.21	0.25	0.91
375	29.24	0.30	0.26	2.34
400	26.54	0.27	0.26	1.85
425	5.28	0.07	0.27	0.01
450	0.39	0.01	0.26	0.001
500	1.12	0.03	0.26	0.009

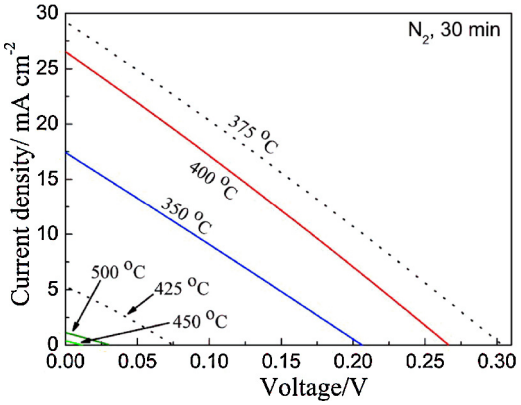

Fig. 6. *J–V* characteristics of CTS absorber layers prepared at various temperatures.

of the CTS by the high temperature annealing as discussed in the XRD and UV–vis-IR data. Among the samples annealed at 350, 400, 450 and 500 °C, the one prepared at 400 °C shows best photovoltaic characteristics.

Since the CTS is sensitive to the annealing temperature, samples with annealing temperatures around 400 °C (at 375 and 425 °C) were also prepared, and their photovoltaic characteristics are shown together in Fig. 6 and Table 1. As observed in Fig. 6 or Table 1, the CTS absorber layer annealed at 375 °C shows best performance among all the prepared samples, and its J_{sc}, V_{oc}, fill factor (FF) and conversion efficiency are 29.24 mA/cm^2, 300 mV, 0.26 and 2.34%, respectively. The high conversion efficiency of the CTS solar cell may be due to the good p–n junction as shown in Fig. 5. However, to further improve the conversion efficiency of the solar cell, the formation mechanism of the p–n junction between the CTS absorber layer and the In_2S_3 buffer layer during the annealing process should be further understood.

4. Conclusion

We have studied the photovoltaic properties of the novel CTS material by employing a superstrate solar cell structure of Mo/CTS/In_2S_3/TiO_2/FTO glass. The CTS powder synthesized by mechanochemical ball milling process was found to be with the preferential orientation along the (1 0 2) plane. The optical and electronic properties of the CTS were easily affected by the annealing temperature. The J_{sc}, V_{oc}, fill factor and conversion efficiency of the best fabricated solar cell are 29.24 mA/cm^2, 300 mV, 0.26 and 2.34%, respectively. Therefore, the CTS material, with abundant and non-toxic constituent elements, has great potential for low cost solar cell application.

To further promote the solar cell conversion efficiency, the quality of the CTS absorber layer should be improved. This study may offer meaningful insight into the promising Cu–Sn–S system photovoltaic materials for low-cost power generation.

Acknowledgment

This work was supported by the Shanghai Committee of Science and Technology, China (Grant No. 10540500700 and 13JC1404300).

References

[1] P. Jackson, D. Hariskos, E. Lotter, S. Paetel, R. Wuerz, R. Menner, W. Wischmann, M. Powalla, New world record efficiency for Cu(In,Ga)Se_2 thin-film solar cells beyond 20%, Prog. Photovolt. Res. Appl. 19 (2011) 894–897.
[2] R.A. Joshi, V.S. Taur, R. Sharma, Effect of annealing on conversion efficiency of nanostructured CdS/$CuInSe_2$ heterojunction thin film solar cell prepared by chemical ion exchange route at room temperature, Mater. Res. Bull. 47 (2012) 2206–2211.
[3] T. Nakada, M. Mizutani, 18% Efficiency Cd-free Cu(In,Ga)Se_2 thin-film solar cells fabricated using chemical bath deposition (CBD)-ZnS buffer layers, Jpn. J. Appl. Phys. 41 (2002) L165–L167.
[4] H. Katagiri, K. Jimbo, W.S. Maw, K. Oishi, M. Yamazaki, H. Araki, A. Takeuchi, Development of CZTS-based thin film solar cells, Thin Solid Films 517 (2009) 2455–2460.
[5] H. Katagiri, K. Jimbo, S. Yamada, T. Kamimura, W.S. Maw, T. Fukano, T. Ito, T. Motohiro, Enhanced conversion efficiencies of Cu_2ZnSnS_4-based thin film solar cells by using preferential etching technique, Appl. Phys. Express 1 (2008) 041201.
[6] I.D. Olekseyuk, I.V. Dudchak, L.V. Piskach, Phase equilibria in the Cu_2S–ZnS–SnS_2 system, J. Alloys Compd. 368 (2004) 135–143.
[7] S. Fiechter, M. Martinez, G. Schmidt, W. Henrion, Y. Tomm, Phase relations and optical properties of semiconducting ternary sulfides in the system Cu–Sn–S, J. Phys. Chem. Solids 64 (2003) 1859–1862.
[8] D. Avellaneda, M.T.S. Nair, P.K. Nair, Cu_2SnS_3 and Cu_4SnS_4 thin films via chemical deposition for photovoltaic application, J. Electrochem. Soc. 157 (2010) D346–D352.
[9] B. Li, Y. Xie, J. Huang, Y. Qian, Synthesis, characterization, and properties of nanocrystalline Cu_2SnS_3, J. Solid State Chem. 153 (2000) 170–173.
[10] X. Chen, H. Wada, A. Sato, M. Mieno, Synthesis, electrical conductivity, and crystal structure of $Cu_4Sn_7S_{16}$ and structure refinement of Cu_2SnS_3, J. Solid State Chem. 139 (1998) 144–151.
[11] M. Bouaziz, J. Ouerfelli, S.K. Srivastava, J.C. Bernede, M. Amlouk, Growth of Cu_2SnS_3 thin films by solid reaction under sulphur atmosphere, Vacuum 85 (2011), 783-186.
[12] P.A. Fernandes, P.M.P. Salome, A.F. Cunha da, A study of ternary Cu_2SnS_3 and Cu_3SnS_4 thin films prepared by sulfurizing stacked metal precursors, J. Phys. D: Appl. Phys. 43 (2010) 215403.
[13] Q.M. Chen, X.M. Dou, Z.Q. Li, S.Y. Cheng, S.L. Zhuang, Printed ethyl cellulose/$CuInSe_2$ composite light absorber layer and its photovoltaic effect, J. Phys. D: Appl. Phys. 44 (2011) 455401.
[14] S.S. Razavi Tousi, R. Yazdani Rad, E. Salahi, I. Mobasherpour, M. Razavi, Production of Al–20 wt.% Al_2O_3 composite powder using high energy milling, Powder Technol. 192 (2009) 346–351.
[15] L. Kavan, M. Gratzel, Highly efficient semiconducting TiO_2 photoelectrodes prepared by aerosol pyrolysis, Electrochim. Acta 40 (1995) 643–652.
[16] T.T. John, S. Bini, Y. Kashiwaba, T. Abe, Y. Yasuhiro, C.S. Kartha, K.P. Vijayakumar, Characterization of spray pyrolysed indium sulfide thin films, Semicond. Sci. Technol. 18 (2003) 491–500.
[17] M. Kaelin, D. Rudmann, A.N. Tiwari, Low cost processing of CIGS thin film solar cells, Sol. Energy 77 (2004) 749–756.
[18] A. Redinger, S. Siebentritt, Coevaporation of $Cu_2ZnSnSe_4$ thin films, Appl. Phys. Lett. 97 (2010) 092111.
[19] A. Redinger, D.M. Berg, P.J. Dale, S. Siebentritt, The consequences of kesterite equilibria for efficient solar cells, J. Am. Chem. Soc. 133 (2011) 3320–3323.
[20] J.J. Scragg, T. Ericson, T. Kubart, M. Edoff, C. Platzer-Bjorkman, Chemical insights into the instability of Cu_2ZnSnS_4 films during annealing, Chem. Mater. 23 (2011) 4625–4633.
[21] D.V. Alexis, Detailed balance limit of the efficiency of tandem solar cells, J. Phys. D: Appl. Phys. 13 (1980) 839–846.
[22] G.H. Moh, Tin-containing mineral systems. Part I: the Sn–Fe–S–O system and mineral assemblages in ores, Chemie der Erde 33 (1974) 243–273.
[23] M.T.S. Nair, L. Guerrero, P.K. Nair, Conversion of chemically deposited CuS thin films to $Cu_{1.8}S$ and $Cu_{1.96}S$ by annealing, Semicond. Sci. Technol. 13 (1998) 1164–1169.
[24] M. Bar, N. Barreau, F. Couzinie-Devy, S. Pookpanratana, J. Klaer, M. Blum, Y. Zhang, W. Yang, J.D. Denlinger, H.W. Schock, L. Weinhardt, J. Kessler, C. Heske, Nondestructive depth-resolved spectroscopic investigation of the heavily intermixed In_2S_3/Cu(In,Ga)Se_2 interface, Appl. Phys. Lett. 96 (2010) 184101.